RSC Advances

ROYAL SOCIETY OF CHEMISTRY

www.rsc.org/advances

Journal Name

ARTICLE

Photoelectric properties of reduced-graphene-oxide film and its photovoltaic application

Received 00th January 20xx,

Accepted 00th January 20xx

DOI: 10.1039/x0xx00000x

www.rsc.org/

Hang He, Xuegong Yu*, Yichao Wu, Haiyan Zhu, Xinhui Mu, Deren Yang

Graphene (Gr) film grown by chemical vapor deposition (CVD) method has recently received intensive attention in optoelectronic devices. As an alternative, the low cost graphene-oxide (GO) fabricated by solution process is more promising for practical application. Here, we have fabricated GO film on copper foil and then reduced it into a conductive film by high temperature annealing. It is found that the photoelectric properties of the reduced-graphene-oxide (r-GO) film are strongly dependent on the annealing temperature and film thickness. A thicker r-GO film under higher temperature annealing usually has better conductivity. By optimizing the reduction conditions of GO films, the highest power conversion efficiency (PCE) of 3.36% can be achieved for a r-GO/Si solar cell. This value is currently the record efficiency for the r-GO/Si device architecture.

Introduction

Graphene film grown by CVD[1] is an extremely promising material in many technological fields such as gas sensors,[2] transparent electrodes[3] and ultrafast photodetectors.[4] Among these applications, Gr combining with silicon to form a solar cell has recently attracted intensive attention. The graphene/silicon (Gr/Si) solar cell can be fabricated by simply transferring a Gr film onto n-type Si substrate at room temperature. In such a solar cell, the Gr film serves as the transparent electrode and introduces a built-in electric field near the interface of Gr/Si. The first reported Gr/Si solar cell has achieved an efficiency of 1.5%.[5] Nature of the Schottky junction has been deeply investigated.[6-8] For performance enhancement, many methods have been employed, such as nanowires[9], sulfide treatment[7] and top-grid structure[10]. Subsequently, considerable progress has been gained and the efficiency of Gr/Si solar cell employing a pristine monolayer Gr has reached nearly 4%.[11] Furthermore, the chemical-doping has been used to tune the work function of Gr films and therefore improve the efficiency of Gr/Si solar cells. For instance, an efficiency of 8.6% has already been reported for the monolayer Gr/Si solar cell by doping the Gr film with bis(trifluoromethanesulfonyl)-amide [$(CF_3SO_2)_2NH$] (TFSA).[12] The maximal PCE of ~14.5% up to now has been achieved for the Gr/Si solar cell by combining HNO_3 doping and TiO_2 antireflection layer.[11] Thus, it is suspected that Gr/Si solar cells could become a potential alternative to the conversional *p-n* junction silicon solar cells.

Compared to CVD-grown Gr films, the GO has the advantage of lower cost and more productivity, which can be simply fabricated with purified natural graphite by the Hummers method.[13] Even though the GO flakes are not electrically conductive, they can be reduced into r-GO flakes by thermal annealing.[14] This point is appealing for the practical application of the GO flakes since they can be easily suspended in aqueous [15] and deposited on a wide range of substrates to form a film. By now, various fabrication methods of r-GO films have been developed, including spin-[14] or spray-coating[16], vacuum filtration technique[17] and electrophoretic deposition.[18] Recently, r-GO films have been used to fabricate the r-GO/Si heterojunction solar cells, and their PCE has reached ~ 2%.[19-21] These results shed the light on the fabrication of high efficiency r-GO/Si solar cells, in which the photoelectric properties of r-GO films are quite critical.

In this paper, we firstly form the GO film on a copper foil and then optimize the photoelectric properties of r-GO film by tuning thermal annealing conditions. The r-GO film was transferred onto n-Si substrate to form a heterojunction solar cell. As observed, the device performance is strongly dependent on the charge transport efficiency in the r-GO film. The highest PCE obtained for the r-GO/Si based devices has reached 3.36%, which is doubly as high as the previously reported values. [19-21]

Experimental details

The GO film was formed by spin-coating the GO solution (1 mg/ml) on a copper foil with a rate of 4000 rpm for one cycle. The thickness of GO films could be modified by simply controlling the spin-coating cycles, which was measured by a step profiler. A 150 °C baking was used to stabilize the film between two spin-coating cycles. Afterwards, the GO films were reduced by thermal annealing for 2 hours in H_2/Ar (V/V=1:1) at the temperature range of 750~1050 °C. The scanning electron microscope (SEM) image was characterized by a SEM (Hitachi S-4800). Atomic Force Microscopy (AFM) (Bruker, Multimode-8) image was taken for a r-GO film

transferred onto a quartz substrate. The carbon content of the GO and r-GO films were probed by taking narrow scans of the C1s region using X-ray photoelectron spectroscopy (XPS, Thermo Fisher Scientific Escalab 250Xi). The Raman spectra of the GO and r-GO films were measured by using a Raman Spectrometer (Bruker, Senterra) with 532 nm diode laser excitation on a 300 lines/mm grating at room temperature. The r-GO films can be transferred to any substrate by a traditional PMMA assisted process.[22] The PMMA was spin coated onto the surface of the r-GO film at 4000 rpm for 30 s, followed by curing at 150 °C for 10 min. The Cu foil was etched away using a mixture of $FeCl_3$ and HCl solution to obtain the PMMA supported r-GO film. Subsequently, the PMMA/r-GO film was rinsed in DI water for 3 times, and then transferred onto the silicon substrate. Finally, the PMMA was removed by annealing under 400 °C for 30 min in Ar/H_2 atmosphere.

After the r-GO films were transferred onto the quartz, the optical transmission spectra of r-GO films were measured by a UV-VIS-NIR spectrophotometer (UV-3600) and the sheet resistance (R_{sheet}) of r-GO films by a four-probe system. For the solar cell fabrication, the r-GO film with a size of 7×7 mm^2 was transferred onto n-Si substrate with a resistivity of 1-3 Ω cm, and then the Ag top electrode was evaporated on the r-GO film to form a 3×3 mm^2 window by using a defined mask, and the back contact was made by scratching InGa eutectic alloy. The detailed process of film fabrication and solar cell assembly is also shown by Fig. 1. The cross-section of the solar cells was characterized by a Transmission Electron Microscopy (TEM) (Tecnai F20 S-TWIN). The current-voltage (*I-V*) characteristics of r-GO/Si solar cells were recorded using a Keithley 4200 Semiconductor Characterization system. The photovoltaic effects of the devices were tested with a solar simulator under conditions of air mass 1.5 (AM 1.5) illumination.

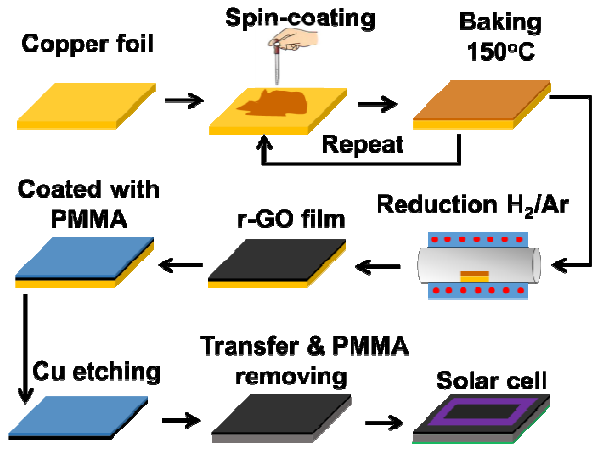

Figure 1 Flow chart of r-GO film fabrication and solar cell assembly processes.

Results and discussion

Fig.2 (a) shows a scanning electron microscopy (SEM) micrograph of r-GO film with 20-cycled spin-coating on a Cu foil after 950 °C annealing. It can be seen that the r-GO flakes indeed form a continuous and uniform film on the Cu foil. The formation of uniform r-GO film should be ascribed to the hydrophilic character of GO, which is particularly suitable for spin-coating technique. The thickness of r-GO film subjected to 20-cycled spin-coating is 18 nm (shown in Fig.S1), which indicates that the thickness of r-GO film with 1-cycled is averagely 0.9 nm. Fig.S2 shows the surface image for 18 nm r-GO film after 950 °C annealing, in which smooth surface morphology is observed, with a small root-mean-square roughness of 1.62 nm. Fig.S3 shows the high resolution C1s XPS peaks of the original GO and r-GO films with a thickness of 18 nm, respectively. Three most prominent deconvoluted components of the C1s envelope can be seen in each panel, which correspond to C-C (284.8 eV), C-O (286.2 eV), C=O (287.8 eV), respectively.[23] Compared to the original GO film with a 65% C-C bonds percentage, seeing Fig.S3 (a), all the r-GO films possess a higher C-C bond percentage. Fig.2 (b) presents the correlation of C-C bond percentage of r-GO films with the reduction temperatures, which is derived from the XPS analysis for the 18 nm r-GO films after 750-1050 °C annealing. It can be seen that a higher temperature annealing can generate a higher C-C percentage for r-GO film. This result reveals that oxygen-containing groups have been gradually removed during the annealing.

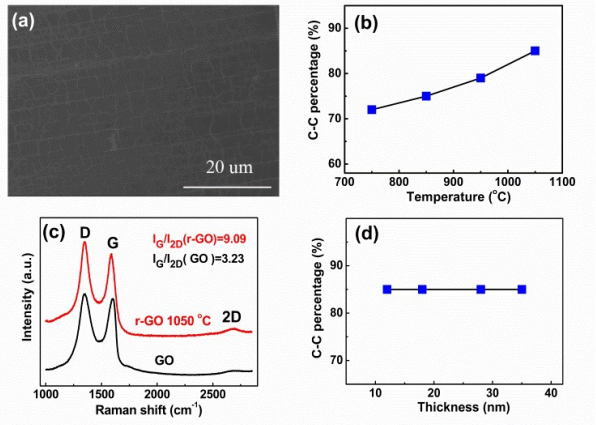

Figure 2 (a) SEM micrograph (plan view) of r-GO film on a copper foil after 950 °C annealing for the 18 nm r-GO film. (b) C-C bond percentage for 18 nm r-GO films after 750-1050 °C annealing derived from XPS analysis. (c) Raman spectra of the original GO film and 18 nm r-GO film after 1050 °C annealing. (d) Result derived from XPS analysis for C-C bond percentage for thickness of 12, 18, 28 and 35 nm under 1050 °C.

Fig.2 (c) shows the Raman spectra of the GO film with a thickness of 18 nm before and after 1050 °C annealing. It can be seen that the typical D band (1330 cm^{-1}) and G band (1588 cm^{-1}) in the Raman spectra exist for both kinds of the films, but

the 2D band (2685 cm^{-1}) only appears for the r-GO film. The increase in magnitude I_G/I_{2D} is indicative of reduction of the GO film.[24] Fig.2 (d) shows the C-C bond percentage of the r-GO films with thicknesses of 12~35 nm after thermal reduction under 1050 °C, which is extracted from the XPS analysis in Fig.S4. It can be seen that the C-C content of r-GO film is mainly determined by the reduction temperature, independent of the film thickness. All these results indicate that the reconstruction of r-GO films indeed takes place during the reduction process of GO films.

Fig. 3(a) shows the photoelectric properties of r-GO films with a thickness of 18 nm after annealing in the temperature 750-1050 °C. It can be seen that the higher optical transmittance (at the wavelength of 550 nm) is achieved for the r-GO film subjected to the higher temperature annealing, reflecting the reduction degree of r-GO film. The R_{sheet} of r-GO films decreases from 9.44 to 3.04 kΩ/cm^2 with the annealing temperature increasing. It is obvious that the conductivity of r-GO films is mainly dependent on the content of carbon unbound with oxygen. Fig. 3(b) shows the photoelectric properties for the r-GO film with thicknesses of 12-35 nm after 1050 °C annealing. It can be seen that both the R_{sheet} and transmittance of r-GO films decrease with the increase of film thickness. A lowest R_{sheet} of 0.53 kΩ/cm^2 has been obtained for the 35 nm thick r-GO film, with the transmittance of 34%. The highest optical transmittance, 84.2%, is achieved for the 12 nm thick r-GO, but the R_{sheet} dramatically increases to 8.37 kΩ/cm^2. Nevertheless, it should be noticed that all these r-GO films shows a transmittance of 30~85% in the visible-light wavelength range. Fig.3 (c) shows the photographs of original GO and r-GO films after 1050 °C annealing on quartz plate with thicknesses of 12~35 nm. It indicates that all the r-GO films are basically transparent.

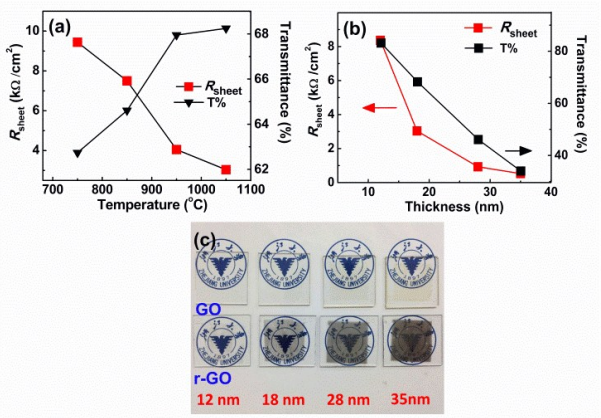

Figure 3 (a) R_{sheet} and transmittance (T%, 550 nm) of 18 nm r-GO films as a function of reduction temperature. (b) R_{sheet} and transmittance (T%, 550 nm) of r-GO films as a function of film thickness. (c) Photograph of the original GO films and r-GO films after 1050 °C annealing on quartz plates with thicknesses of 12-35 nm.

Generally, the ratio of direct current and optical conductivity (σ_{dc}/σ_{op}) can be used as a figure-of-merit to evaluate the photoelectric performance of transparent conductors,[25] which can be expressed as

$$\frac{\sigma_{op}(\lambda)}{\sigma_{dc}} = \frac{2R_{sheet}}{273}\left(\frac{1}{T(\lambda)^2} - 1\right) \quad (1)$$

where $T(\lambda)$ is the transmittance (λ=550 nm) and R_{sheet} the sheet resistance of the transparent conductor. Fig.4 (a) shows the σ_{dc}/σ_{op} values for the 18 nm r-GO films after annealing under different temperatures. Note that a high σ_{dc}/σ_{op} value means that the transparent conductor film has superior photoelectric properties. One can see that the σ_{dc}/σ_{op} values of r-GO films, which are markedly dependent of annealing temperature, can reach a larger value under higher temperature. Fig.4 (b) shows the σ_{dc}/σ_{op} values of r-GO films with thicknesses of 12-35 nm after 1050 °C annealing. It can be seen that the σ_{dc}/σ_{op} values of r-GO films, which are dependent of the film thickness, can reach a maximal value of 0.054 for the 28 nm thick r-GO film.

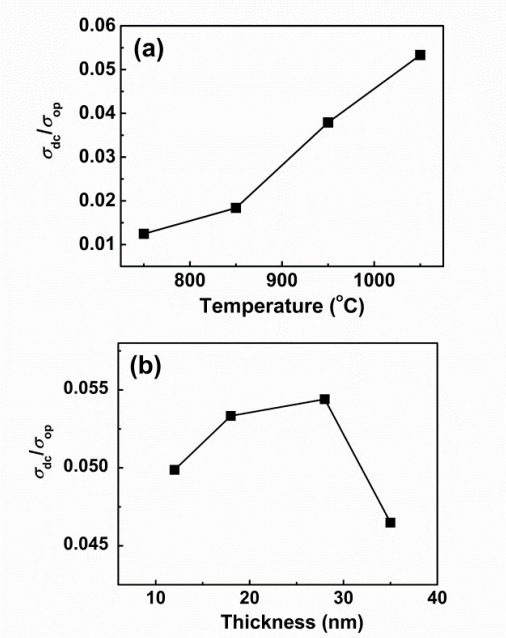

Figure 4 (a) Values of σ_{dc}/σ_{op} for the 18 nm r-GO films after annealing under different temperatures. (b) Values of σ_{dc}/σ_{op} for the r-GO films after 1050 °C annealing with various thicknesses.

If combining the r-GO film with n-Si to form a solar cell, the corresponding energy diagram near the r-GO/n-Si interface can be shown by Fig.5 (a). Theoretically, a build-in potential is produced in n-Si adjacent to the interface due to the different work functions of r-GO and n-Si. The space-charge region is therefore formed accompanied by the build-in potential (V_i) in the Si part near the interface. Under sunlight illumination, the photon-generated carriers are separated and subsequently collected by the electrodes, yielding photovoltaic effects.

Fig.5 (b) shows a typical cross-section TEM image of the fabricated r-GO/Si cell. It can be seen that the r-GO film is tightly anchored onto the silicon substrate, which is attributed

to the 400 °C annealing process for removing PMMA. Fig.5 (c) shows the current density-voltage (*J-V*) curves of the fabricated r-GO/n-Si solar cells with 18 nm r-GO films via different annealing temperatures under AM 1.5. It can be seen that all these devices exhibit significant photovoltaic effect, suggesting that a Schottky junction is indeed formed at the interface of r-GO and n-Si. The corresponding parameters of solar cells are shown in Fig.5 (d). One can see that devices with r-GO film obtained via different annealing temperatures exhibit a comparable open-circuit voltage (V_{oc}) of ~ 0.45 V, indicating that the Schottky junction barrier remain nearly the same though these r-GO films were obtained under annealing in 750-1050 °C. The filling factor (FF) shows a slight variation between 22.72% and 29.84% with the increase of the annealing temperature. It's worth noting that, the short-circuit current density (J_{sc}) of r-GO/Si solar cells get obviously increased from 10.24 to 22.12 mA/cm^2 with the increase of film annealing temperature. Therefore, the performances of cells increase with the observably increased J_{sc}. This result is in accordance with the values of σ_{dc}/σ_{op} for the 18 nm r-GO films after annealing under different temperatures.

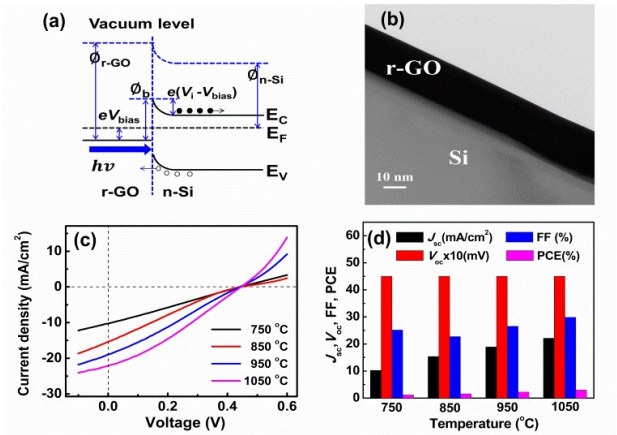

Figure 5 (a) The energy band diagram of r-GO/n-Si solar cells at the interface under illumination. E_C, E_V, E_F correspond to the conduction band edge, valence band edge, and Fermi level of n-Si, respectively. $\emptyset_b$: potential barrier; $e(V_i\text{-}V_{bias})$: built-in field; $\emptyset_{r\text{-}GO}$: work function of r-GO; $\emptyset_{n\text{-}Si}$: work function of n-Si. (b) A typical cross-section TEM image of the fabricated r-GO/Si cell. (c) Illuminated *J-V* curves of cells with 18 nm r-GO films after annealing under different temperatures (AM 1.5). (d) Parameters of solar cells in (c).

Fig.6 (a) shows the illuminated *J-V* curves of the fabricated r-GO/n-Si solar cells. Note that the r-GO films with thicknesses of 12-35 nm were obtained by 1050 °C annealing here. It can be seen that all these devices exhibit significant photovoltaic effect, suggesting that a Schottky junction is indeed formed at the interface of r-GO and n-Si. The corresponding parameters of solar cells are shown in Fig.6 (b). One can see that devices with different r-GO film thickness exhibit a comparable V_{oc} of ~ 0.45 V. The FF shows an obvious increase from 26.65% to 36.45% with the increase of the r-GO film thickness, corresponding to the decrease of the film R_{sheet}. More interestingly, the J_{sc} of r-GO/Si solar cells also increases from 15.76 to 20.48 mA/cm^2 with the increase of r-GO film thickness. However, the thickness of r-GO film reaches 35 nm, the performances of solar cell performance start to deteriorate. As a result, the highest PCE of 3.36% can be obtained for the r-GO/Si solar cell using a 28 nm thick r-GO film. The series resistance (R_s) of the r-GO/Si solar cells can be extracted by plotting the curve of dV/dln$I$ as a function of I, based on the following relationship,[26]

$$I = I_0 \exp(\frac{e(V - IR_s)}{nkT}) \quad (2)$$

The inset of Fig.6 (c) shows the linear fitting of these curves and the calculated values of R_s for all the solar cells are shown in Fig.6 (c). It can be seen that the solar cell based on a thicker r-GO film possesses a lower R_s, which is consistent with the variation in the R_{sheet} of the r-GO film.

As for the thickness-dependent performance, it is reasonable to assume that the relation of device performance to r-GO active layer is dominated by two parameters, the R_{sheet} of r-GO layer and the transparency of r-GO, which are responsible for the carrier transport efficiency and light transmission efficiency, respectively. For the r-GO film with high transmittance, the J_{sc} of r-GO/Si solar cell is mainly restricted by the R_{sheet} of r-GO. Therefore, the J_{sc} of solar cells increases with a decrease of R_{sheet} of r-GO. When the r-GO film becomes much thicker, the light transmission efficiency is dramatically weak, which suppresses the device performance improvement. The trade-off between the carrier transport efficiency and light transmission efficiency is achieved for the r-GO film with a thickness of 28 nm, which results in the highest efficiency for the r-GO/Si solar cell.

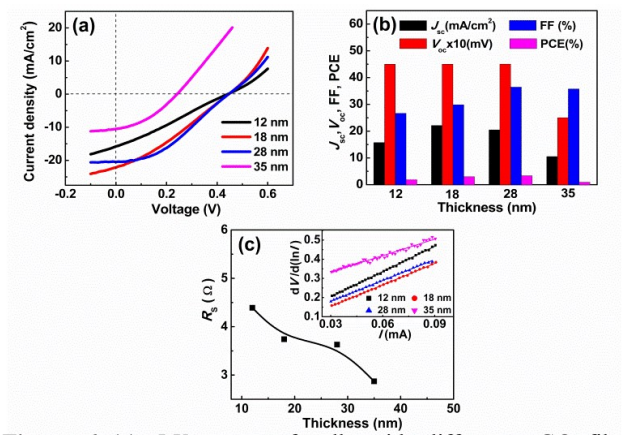

Figure 6 (a) *J-V* curves of cells with different r-GO film thickness under AM 1.5. (b) Parameters of solar cells in (a). (c) Series resistance of cells with different r-GO film thickness as a function of r-GO film thickness, inset shows the calculation of R_s.

Finally, we have compared the performances of our r-GO/Si based on the 28 nm thick r-GO film with those of the control GO/Si and CVD-Gr/Si solar cells prepared by the same transfer process. In the CVD-Gr/Si solar cell, the Gr is a monolayer

graphene film. Fig.7 shows the illuminated *J-V* curves of the GO/Si, CVD-Gr/Si and r-GO/Si devices, and the detailed parameters of the GO/Si, CVD-Gr/Si, r-GO/Si devices are shown in Table S1. It can be seen that no obvious photovoltaic effect occurs for the GO/Si device. This result indicates that GO film before annealing is not suitable for the solar cell fabrication. For the CVD-Gr/Si solar cell, the J_{sc}, V_{oc} and *FF* are 10.86 mA/cm^2, 370 mV and 49.52%, respectively, and therefore a PCE of 1.99% has been achieved. Compared to CVD-Gr/Si device, the r-GO/Si device with an efficiency of 3.36% shows superior photovoltaic performances, which is attributed to higher J_{sc} and V_{oc}. This result demonstrates that the low-cost r-GO/Si cell could act as an alternative for the CVD-Gr/Si cell.

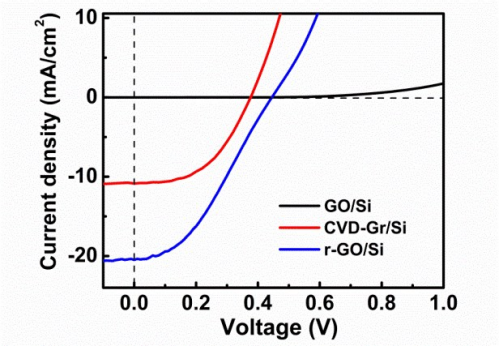

Figure 7 *J-V* curves of the GO/Si, CVD-Gr/Si and optimized r-GO/Si devices under AM 1.5.

Conclusions

In summary, we have prepared the r-GO films with different thicknesses by annealing. It is found that the photoelectric properties of the r-GO films are strongly dependent on both annealing temperature and film thickness. As for the temperature-dependent performance, high annealing temperature is beneficial for obtaining r-GO film with high photoelectric properties, which results in high performance cell. As for the thickness-dependent performance, there exists a trade-off between film conductivity and transmittance for optimizing photoelectric properties of r-GO film in photovoltaic application. When the thickness of r-GO film is smaller than 28 nm, the conductivity of r-GO film is dominant in the solar cell performance. However, with an increase of the r-GO film thickness, the transparency of r-GO film plays a more important role in the solar cell performance. The highest efficiency of 3.36% can be obtained for the r-GO/Si solar cell using a 28 nm thick r-GO film obtained by 1050 ^{o}C annealing. This value is currently the record efficiency for the r-GO/Si solar cells.

Acknowledgements

This work is supported by the National Natural Science Foundation of China (Nos. 61422404 and 51472219) and the Program for Innovative Research Team in University of Ministry Education of China (IRT13R54).

Notes and references

State Key Laboratory of Silicon Materials
Department of Materials Science and Engineering
Zhejiang University
Hangzhou 310027, People's Republic of China.
E-mail: yuxuegong@zju.edu.cn

1.X. Li, W. Cai, J. An, S. Kim, J. Nah, D. Yang, R. Piner, A. Velamakanni, I. Jung, E. Tutuc, S. K. Banerjee, L. Colombo and R. S. Ruoff, *Science*, 2009, **324**, 1312.
2.G. Lu, L. E. Ocola and J. Chen, *Appl. Phys. Lett.*, 2009, **94**, 083111.
3.K. S. Kim, Y. Zhao, H. Jang, S. Y. Lee, J. M. Kim, K. S. Kim, J. H. Ahn, P. Kim, J. Y. Choi and B. H. Hong, *Nature*, 2009, **457**, 706.
4.Y. An, A. Behnam, E. Pop and A. Ural, *Appl. Phys. Lett.*, 2013, **102**, 013110.
5.X. Li, H. Zhu, K. Wang, A. Cao, J. Wei, C. Li, Y. Jia, Z. Li, X. Li and D. Wu, *Adv. Mater.*, 2010, **22**, 2743.
6.Y. J. Lin and J. H. Lin, *Appl. Surf. Sci.*, 2014, **311**, 224.
7.Y. J. Lin and J. J. Zeng, *Appl. Surf. Sci.*, 2014, **322**, 225.
8.Z. Arefinia and A. Asgari, *Mat. Sci. Semicon. Proc.*, 2015, **35**, 181.
9.Z. Arefinia and A. Asgari, *Sol. Energ. Mat. Sol. C.*, 2015, **137**, 146.
10.Y. Wang, C. Chen, X. Fang, Z. Li, H. Qiao, B. Sun and Q. Bao, *J. Solid State Chem.*, 2015, **224**, 102.
11.E. Shi, H. Li, L. Yang, L. Zhang, Z. Li, P. Li, Y. Shang, S. Wu, X. Li, J. Wei, K. Wang, H. Zhu, D. Wu, Y. Fang and A. Cao, *Nano Lett.*, 2013, **13**, 1776.
12.X. Miao, S. Tongay, M. K. Petterson, K. Berke, A. G. Rinzler, B. R. Appleton and A. F. Hebard, *Nano Lett.*, 2012, **12**, 2745.
13.D. A. Dikin, S. Stankovich, E. J. Zimney, R. D. Piner, G. H. Dommett, G. Evmenenko, S. T. Nguyen and R. S. Ruoff, *Nature*, 2007, **448**, 457.
14.H. A. Becerril, J. Mao, Z. Liu, R. M. Stoltenberg, Z. Bao and Y. Chen, *ACS Nano*, 2008, **2**, 463.
15.S. Stankovich, R. D. Piner, X. Chen, N. Wu, S. T. Nguyen and R. S. Ruoff, *J. Mater. Chem.*, 2006, **16**, 155.
16.V. H. Pham, T. V. Cuong, S. H. Hur, E. W. Shin, J. S. Kim, J. S. Chung and E. J. Kim, *Carbon*, 2010, **48**, 1945.
17.G. Eda, G. Fanchini and M. Chhowlla, *Nat. Nanotechnol.*, 2008, **3**, 270.
18.Z. S. Wu, S. Pei, W. Ren, D. Tang, L. Gao, B. Liu, F. Li, C. Liu and H. M. Cheng, *Adv. Mater.*, 2009, **21**, 1756.
19.L. Chen, H. He, H. Yu, Y. Cao and D. Yang, *Electrochim. Acta*, 2014, **130**, 279.
20.S. K. Behura, S. Nayak, I. Mukhopadhyay and O. Jani, *Carbon*, 2014, **67**, 766.

21.Z. Li, L. Zheng, V. Saini, S. Bourdo, E. Dervishi and A. S. Biris, *J. Exp. Nanosci.*, 2013, **8**, 565.
22.X. Li, Y. Zhu, W. Cai, M. Borysiak, B. Han, D. Chen, R. D. Piner, L. Colombo and R. S. Ruoff, *Nano Lett.*, 2009, **9**, 4359.
23.Y. Zhu, W. Cai, R. D. Piner, A. Velamakanni and R. S. Ruoff, *Appl. Phys. Lett.*, 2009, **95**, 103104.
24.D. Yang, A. Velamakanni, G. Bozoklu, S. Park, M. Stoller, R. D. Piner, S. Stankovich, I. Jung, D. A. Field, C. A. Ventrice and R. S. Ruoff, *Carbon*, 2009, **47**, 145.
25.M. Song, D. S. You, K. Lim, S. Park, S. Jung, C. S. Kim, D. H. Kim, D. G. Kim, J. K. Kim, J. Park, Y. C. Kang, J. Heo, S. H. Jin, J. H. Park and J. W. Kang, *Adv. Funct. Mater.*, 2013, **23**, 4177.
26.W. Jie, F. Zheng and J. Hao, *Appl. Phys. Lett.*, 2013, **103**, 233111.